AERODYNAMIC LOADS AND BLADE VORTEX INTERACTION

NOISE PREDICTION

BY

M. SCHAFFAR,J. HAERTIG AND P. GNEMMI

INSTITUT FRANCO-ALLEMAND DE RECHERCHES DE SAINT-LOUIS

68301 SAINT-LOUIS , FRANCE

FIFTEENTH EUROPEAN ROTORCRAFT FORUM

SEPTEMBER 12 - 15, 1989 AMSTERDAM

AERODYNAMIC LOADS AND BLADE VORTEX INTERACTION
NOISE PREDICTION

M. SCHAFFAR, J. HAERTIG, P. GNEMMI

Institut Franco-Allemand de Recherches de Saint-Louis
12 rue de l'industrie
68301 SAINT-LOUIS (France)

Abstract

The vortex lattice method is described and applied in order to predict the aerodynamic loads on a thin two-bladed rotor. A local conformal mapping for each position in span is used to transform the thin rotor into a thick one. The pressure coefficients obtained for the thick rotor are fed into an acoustic code which is based on the Ffowcs-Williams-Hawkings (FW-H) equation . The results obtained with this method show the importance of the rotor and flight parameters; they are compared with results found in the literature for a two-bladed rotor in hovering and advancing. The comparison shows a good agreement and exhibits that the cut-off length for limiting the instabilities from the Biot and Savart law must be chosen carefully.

1. Introduction

Rotor blade-vortex interaction (BVI) noise is an important noise source for helicopters in flight. This phenomenon is always present but becomes stronger in descent flight; it has to be reduced and many people are interested in the reduction of this noise. This inter-action noise is caused by unsteady airloads induced on the blades by the vortical wake of previous blades. A good understanding of this complex problem needs mathematical models for computer simulation and noise prediction and windtunnel or in-flight tests for comparison and verification.

Many experimental works have been done on rotor noise in the last ten years. Most of these studies have been achieved in the USA and in Europe (ONERA, DFVLR Braunschweig, NASA Ames). Blade-vortex interaction noise [1 to 4] shows a strong forward directivity with a maximum between 30 and 45° below the rotor plane and exhibits also a great dependence on the rotor operating parameters like advance ratio, tip-path-plane angle and hover tip Mach number. Many theoretical studies have been achieved in the 2D and in the 3D case. At the ISL [5 to 8] methods based on conformal mapping or

linearly distributed vortical singularities have been used to investigate the 2D interaction between a profile and a point vortex. The results obtained by the two methods are comparable. It was found that the vortex strength and the vortex path are the main parameters for the interaction. Comparisons were also made with the lift measured on an airfoil interacting with a line vortex in the water tunnel: the agreement between computation and experiment was reasonable.

In the 3D case we find sophisticated methods (based on Navier-Stokes equations, on the full potential equation or on the unsteady transonic small disturbance equation) and more or less simplified methods based on singularities (vortex panels or vortex lattice). We have chosen the Vortex Lattice Method (VLM), a bound lattice for the blade and a free lattice for the wake; this method seems to be promising because it does not need too much computation capacity.

For the noise prediction, the most commonly used method is based on the Ffowcs-Williams-Hawkings equation which needs the pressure coefficients on the blade.

In the next sections, we will describe the vortex lattice method, then the method used to "thicken" the thin blade. Finally we present the results obtained for a two-bladed rotor hovering and advancing.

2. Description of the computational method

2.1 Description of the VLM

The VLM is an extension to the 3D case of 2D methods based on potential flow with point vortices and the same basic assumptions are made: incompressible and inviscid flow. A good description of this method is given in [9,10]. In the case of a one-bladed rotor, the rectangular blade is divided into $N = N_x \cdot N_y$ rectangular panels ($N_x = 12$ chordwise, $N_y = 14$ spanwise). On each panel (i, j) we put a vortex line in span direction of the strength $\Gamma^n_{i,j}$ (figure 1) and a vortex line in chord direction of the strength $\gamma^n_{i,j}$ defined by:

$$\gamma^n_{i,j} = \sum_{k=1}^{i} (\Gamma^n_{k,j-1} - \Gamma^n_{k,j}) \tag{1}$$

where n indicates the time step.

Two frames of reference are necessary: Oxyz is fixed and Ox'y'z rotates with the blade. The center of rotation O is also fixed and the freestream velocity U_∞ is equal to 1 and

parallel to the x-axis. The no-penetration condition on the blade has to be applied in the moving frame. For more convenience the system is projected into the fixed frame, which gives for the time step n:

$$[\vec{V}_{i,j}(\Gamma^n_{i,j}, \gamma^n_{i,j}) + \vec{V}_{i,j}(\text{wake}) + \vec{\Omega} \wedge \vec{r}_{i,j} + \vec{U}_\infty] \cdot \vec{n}_{i,j} = 0 \tag{2}$$

$$\forall_{i,j} \quad i = 1, N_x$$
$$j = 1, N_y \ .$$

The two first terms in (2) are the velocities induced by the blade-bounded vortices ($\Gamma^n_{i,j}$ and $\gamma^n_{i,j}$) and by the free vortices (wake); $\vec{\Omega} \wedge \vec{r}_{i,j}$ is the rotation velocity at the control point of the panel (i,j). At each time step the conservation of the circulation is warranted by the shedding of an unsteady vortex line β^n.

The wake lattice is built stepwise with the vortices β_i^{k} and γ_i^{k} (previously shedded) whose circulation remains constant. The solution of the problem is obtained by solving the system of N linear equations resulting from the condition of no-penetration applied at the control point x_c of each panel. To obtain a good approximation, the rule of Pistolesi is followed (1/4, 3/4, figure 2) although its validity was only demonstrated [11] in the 2D case.

The system is built by writing the induced velocities at each control point. The Biot-Savart law gives the induced velocity for a line vortex (figure 3):

$$\vec{V}_{\text{ind}} = \frac{\Gamma}{4\pi} \frac{(\cos \alpha + \cos \beta)}{r} \frac{\vec{AB} \wedge \vec{AM}}{|\vec{AB} \wedge \vec{AM}|} \ . \tag{3}$$

The pressure jump across the airfoil $\Delta p_{i,j} = -(p_\ell - p_u)_{i,j}$ is obtained with the Bernouilli equation written for the upper (u) and the lower (ℓ) side of the wing:

$$-\left(\frac{p_\ell - p_u}{\rho}\right)_{i,j} = \left[-\frac{\partial(\varphi_u - \varphi_\ell)}{\partial t} + \frac{U_\ell^2 - U_u^2}{2}\right]_{i,j} \tag{4}$$

With the definition of the potential φ and the relation $\vec{u} = \text{grad}\,(\varphi)$ we determine the above expressions by using the singularities $\Gamma_{i,j}$ and $\gamma_{i,j}$.

At the end of the time step n, the normalized rotor thrust coefficient C_T is computed (we take $\rho = 1$) with:

$$C_T(t) = \left(\sum_{i,j} \Delta p_{i,j} S_{i,j}\right) / (\pi R^2 (\Omega R)^2) \ . \tag{5}$$

<u>Note</u>
In the equation (3) we have a source of numerical problems when the distance r is too small. Several regularization methods were tested and the best results (according to MOOK [12]) are obtained when the contribution of the segment is neglected (put to zero) for a distance r smaller than a given threshold (cut-off distance) which needs to be chosen carefully.

2.2 Description of the method used to thicken the blade

The VLM can only be used for lifting surfaces computation whereas acoustic prediction of loading noise based on FW-H equation needs the local loads (strength and direction) acting upon a thick blade.

At each time step the following assumption is made: for each position in span a conformal mapping can be used to extrapolate the results to a thick blade assuming that the potential φ remains the same.

For a given position on the blade (k,j) and using the control point velocities V_x, V_y, V_z and the velocity jump $\Delta \dot{V} = (\dot{U}_u - \dot{U}_\ell)_{k,j}$ expressed in the ground fixed frame, one can calculate the tangential velocity U_T and the transversal velocity U_Y in the blade fixed frame for the upper (u) and for the lower (l) side of the blade.

For each position in span (index j), a conformal mapping can transform the thin blade into a thick Joukowski profile (as an example) of thickness $\approx \varepsilon$, and chord 1. This gives the following complex velocity w in a plane perpendicular to the span (complex plane ξ):

$$\left(w_{u,\ell}\right)_{k,j} = \left(U_{T_{u,\ell}}\right)_{k,j} \times \left[\frac{1}{1+\varepsilon} \left(1 - \frac{\varepsilon}{(\xi_{u,\ell})_k}\right)^{?} \left(1 + \frac{2\varepsilon}{(\xi_{u,\ell})_k + 1 - 2\varepsilon}\right) \right] \tag{6}$$

with $(\xi_{u,\ell})_k = \exp\left(\pm \, i \, \text{Arc} \, \cos \, \sqrt{x_k}\right)$, $x_k = $ chordwise position.

The potential φ is obtained by integrating the velocity along a line coming from infinity , 10 spans in z-direction to the inner TE and by adding (upper side) or by subtracting (lower side) half of the encountered singularity $\Gamma_{\ell,j}$ from one control point to the next.

The pressure coefficient $(C_p)_{u,\ell}$ is then calculated for the upper and the lower side of the "thick" blade.

2.3 BVI noise prediction

Starting from the well-known Ffowcs-Williams-Hawkings equation and following the integration of Lowson, the fluctuation of the acoustic pressure for the loading noise can be expressed with the following equation:

$$4\pi p(\vec{x}, t) = -\int_S \left[\frac{1}{a_0 r (1 - M_r)^2} \left\{ \frac{\partial \ell_r}{\partial \tau} + \ell_r \frac{\frac{\partial M_r}{\partial \tau}}{(1 - M_r)} \right\} \right] dS \tag{7}$$

In the same way, the acoustic pressure for the thickness noise is expressed by:

$$4\pi p(\vec{x}, t) = -\int_S \left[\frac{1}{(1 - M_r)} \frac{\partial}{\partial \tau} \rho_0 \frac{V_n}{r(1 - M_r)} \right] dS \tag{8}$$

where M_r is the Mach number of the element dS relating to the observer, r is the distance between dS and the observer, ℓ_r is the component of the loading vector $\vec{\ell}$ in the observer direction, τ is the emission time ($= t - r/a_0$) at which the terms in [ ], have to be evaluated, a_0 is the sound speed, V_n is the scalar product between the velocity on the blade and the interior normal vector for the surface element dS.

The noise is computed in the time domain with a code similar to the one used by Farrasat [13] which is based on the MIT code for subsonic tip speed propellers.

3. Application to a two-bladed rotor

3.1 Rotor in hover

As a first test , the hovering case was chosen because it has been extensively studied. In the proceedings of previous forums , Favier et al. [14] have presented experimental measurements in good agreement with a free wake computational method. This method is based on a division of the wake into near and far regions which are empirically prescribed according to synthesized laws of contraction and convection obtained experimentally for each region. The computational process consists in an iterative one, starting from the Landgrebe formulation of the circulation on the blade.

The rotor (described as number 7 in ref.14) has following undimensionalized characteristics: chord 1., root distance 3.34, span 11.66, linear twist 8°3, collective pitch 10°, coning angle 3°, no cyclic pitch, rotational angular velocity $\Omega = (0.,0.,.4)$. Figure 4

5

shows the evolution of the thrust coefficient C_T with the azimuth angle $\psi(°)$ for 13.5 rotor revolutions. The first revolutions are clearly recognizable in the step-wise behaviour of the thrust coefficient. After 9 revolutions, the curve tends to a limit, the value of this limit is 0.00446 which is in good agreement with the value of 0.004416 obtained by Favier in the same case (in our calculation, the cut-off length was chosen equal to a half chord).

Figure 5 shows the evolution of the normalized circulation $\dfrac{\Gamma}{(\Omega R^2)}$ ·100. over the blade after 13.5 rotor revolutions in comparison with the experimental points of Favier. The agreement is good up to r/R equal to .9; at the tip of the blade r/R > .9, the measured circulation shows a peak value of 2.8 while the computed value is equal to 1.85. This difference may have its origine in the lifting surface theory used in the VLM, where the tip of the blade is considered as a thin surface, which is not the case for a real blade.

Figure 6 presents the tip vortex trajectories (computed and measured): the axial coordinates z/R and the contraction of the vortex r/R. In this case the agreement between computation and measurement seems to be satisfying .

In conclusion, the VLM seems to be suited for the computation of the main features interesting a rotor in hover although the normalized circulation found near the tip is weaker than the measured one.

3.2 Advancing Rotor

The second test rotor is the two-bladed AH1-OLS rotor which has often been used for acoustic measurements [1]. In this reference, the rotor undimensionalized characteristics are the following: chord 1., rotor radius R = 9.22, root distance 1.678, linear twist 10°, collective pitch 4.73°, coning angle 0°, advancing coefficient μ = 0.164, rotational angular velocity Ω = (0.,0.,0.6632), tip path plane angle 2°, free stream velocity equal to 1., thickness coefficient 9.7%.

In reference [1], two types of results are presented: in-flight tests and wind-tunnel tests; for our comparison, we take into account only the wind-tunnel tests (μ = 0.164, C_T = 0.0054, cyclic pitch θ_c = 1°97, θ_s = 1°). It is obvious that with the blade pitch angle varying with the following relation

$\theta = \theta_0 - \theta_c\cos(\psi) - \theta_s\sin(\psi)$,

the time evolution of the thrust coefficient will have a sine shape. Figure 7 shows four cases with different cyclic pitch: 1)no cyclic pitch, 2) $\theta_c = 1°97, \theta_s = 1°$, 3)$\theta_c = 2°97$, $\theta_s = .5°$, 4) $\theta_c = 3°5, \theta_s = 0..$

The effect of the cyclic pitch is obvious: the amplitude of the oscillations decreases with the increase of the cyclic pitch, especially with the value of θ_c. Moreover, the mean value of the thrust coefficient increases with the increase of the cyclic pitch: from 0.00485 (no cyclic pitch) to 0.0054 for the fourth case. The agreement with the experimental value (0.0054) seems to be acceptable. The cases one and four were chosen for acoustic predictions: the first for a basic computation and some special tests, the fourth for its good agreement in the experimental thrust coefficient .

The analysis of the wake shows following features: the peak on the C_T curves for $\psi = 600°$ or 780° or 960° is the sign of an advancing blade vortex interaction, in the same manner the peak for $\psi = 670°$ or 850° corresponds to a retreating blade vortex interaction.

For the noise prediction, all the computations were made with a cut-off length of .5 chord, the effect of another cut-off length will be presented later. Moreover, the velocity of the free stream was taken equal to 37 m/s, the chord to 0.104 m and the observer distance to 1.72 D = 3.30 m according to the values used in reference [1] .

Noise prediction for the case without cyclic pitch

Figure 8 shows the horizontal directivities for the loading noise for several angles below the rotor plane. As we can see in this figure , the maximum of the directivity is obtained for an azimuth angle near 180°. This may correspond with the advancing blade interaction ($\psi = 600, 780$ or 960°). Nevertheless, the retreating blade interaction (for $\psi = 670$ or 850°) is not clearly visible. Figure 9 shows the pressure signature obtained for the maximum at 30° below the rotor plane. The shape of this signature is very similar to the measured signatures (see figure 11) but the positive peak is only half of the measured one (20 Pa in comparison with 40 Pa).

Note

In this case a special test has been made with a cut-off length of .1 chord. In the compu-tation the cut-off length is applied for the velocities induced from the wake on the blades and from the wake on itself. The interaction peaks on the thrust coefficient are higher and the pressure signatures have a positive peak of 45 Pa. Nevertheless, this result can not be taken into account: a fine analysis of the different contributions shows that the interaction noise is produced by irregularities originating from the Biot and Savart law and by the internal (root) vortex (this root vortex may not be realistic and is probably destroyed by the rotor hub).

Another test was made with a higher panel number: 468 panels per blade instead of 168 panels. The result is the following: the mean value of the thrust coefficient C_T is reduced (3%),the shape of the curve is smoothed but the interaction peaks noted before remain the same.

Noise prediction for the case with cyclic pitch

As it was shown previously, the cyclic pitch used here is a little stronger than in the experiment: θ_c is set equal to 3.5° (instead of 1.97°) and θ_s to 0°(instead of 1°). For the computed pressure, the signatures are the sum of the loading noise and the thickness noise. Figure 10 shows the horizontal directivities for several planes in the rotor plane and below. In all cases the maximum of the noise emission is obtained in the forward direction, for θ near 0°. This maximum is probably produced by the advancing blade vortex interaction for $\psi = 240°$. In the rotor plane, the thickness noise seems to be predominent,which is consistent with the experiment on high-speed noise. The noise emission of the retreating blade vortex interaction for $\psi = 130°$ is recognizable in a second lobe in the directivity for θ near 260°.

Figure 11 shows a comparison between our pressure signatures and these obtained by Splettstoesser et al. [1] for the same positions. These results suggest the following remarks:

- the general shape of the calculated signatures shows an acceptable agreement in comparison with the measured signatures, but the relative time position of the strongest peaks is not the same,

- in general, the computed pressures are higher than the measured ones by a factor in-between 1.2 and 1.8,except for $\theta = 0°$ and $\varphi = -30$ and -45°. The source of this difference may be the higher cyclic pitch used for the computation in comparison with the experimental one (see above).

In conclusion, all these results are interesting: they prove that the vortex lattice method is applicable for rotor computation and they show also that the cut-off length is an important parameter. Thus it is necessary to find a "mathematical" or a "physical" way for the choice of this length. Moreover, this method has to be compared with fully three-dimensional methods (especially for the distribution of the circulation at the tip of the blade in the hovering case and for the evolution of the pressure coefficients obtained with the method used to thicken the blade).

4. Concluding remarks

The vortex lattice method explained in this paper seems to be a good compromise between the "super" codes used for solving the Navier-Stokes equations and a normal CPU consumption.

This method was also able to compute a thin two-bladed rotor in hover. The calculated thrust coefficient is in good agreement with the measured one and the tip vortex trajectories agree very well with the measured ones.

Nevertheless, the standard vortex lattice method cannot be applied to thick airfoil computation and thus cannot be used for noise prediction.

To overcome this difficulty an additional conformal mapping was successfully used. This method was applied to a two-bladed rotor for calculating the BVI with its own wake and the computed aerodynamic forces were used to run an acoustic code based on the Ffowcs-Williams-Hawkings equation.

BVI noise prediction was made and the results are comparable with wind-tunnel experiments. In the horizontal plane the maximum noise was found in the forward direction. The order of magnitude of the calculated signatures in the rotor plane and below shows a reasonable agreement with the experimental signatures.

In the future this method (VLM with local conformal mapping) can be applied to a three- or four-bladed rotor. The problem of advanced blade tip can also be studied with the VLM.

BIBLIOGRAPHY

[1] W.R. SPLETTSTOESSER,K.J. SCHULTZ,D.A. BOXWELL and F.H. SCHMITZ
Helicopter model rotor blade vortex interaction impulsive noise: scalability and parametric variation
NASA TM 86007 dec.1894

[2] R.M. MARTIN and W.R. SPLETTSTOESSER
Blade-vortex interaction acoustic results from a forty percent model rotor in the DNW
Journal of the American Helicopter Society, jan.1988, pp37-46

[3] F.H. SCHMITZ,D.A. BOXWELL,S. LEWY and C. DAHAN
A note on the general scaling of helicopter blade-vortex interaction noise
ONERA TP 1982-32,1982

[4] D.R.HOAD
Helicopter blade vortex interaction location: scale model acoustics and free-wake analysis results
NASA Technical Paper 2656 , April 1987

[5] J.HAERTIG
Interaction entre un tourbillon et un profil d'aile (écoulement incompressible 2D)
ISL Report R 119/85, 1985

[6] M.SCHAFFAR
Interaction profil/tourbillon traitée avec la méthode des singularités (écoulement 2D incompressible)
ISL Report R 103/86, 1986

[7] J. HAERTIG,Ch. JOHE and M. SCHAFFAR
Interaction profil/tourbillon
ISL Report R 125/87, 1987

[8] M. CAPLOT and J. HAERTIG
Prediction of rotor blade-vortex interaction noise from 2D aerodynamic calculations and measurements
Fourteenth European Rotorcraft FORUM,Paper No.3,20-23 sept., 1988, Milano,Italy

[9] P.KONSTADINOPOULOS
A vortex-lattice method for general,unsteady,supersonic aerodynamics
M.S.Thesis,Dept.of Engineering,Virginia Polytechnic Institute and State Univ., Blacksburg, Virginia, July 1981

[10] M. SCHAFFAR and J. HAERTIG
Etude de l'interaction pale/tourbillon sur un rotor monopale en vol d'avancement (fluide non-visqueux et incompressible)
ISL Report R 115/88, 1989

[11] R.M.JAMES
On the remarkable accuracy of the vortex lattice method
Computer Methods in Applied Mechanics and Engineering,1, 1972, pp.59-79

[12] D.T.MOOK
Unsteady Aerodynamics
Lecture series 1988-07,Von Kàrmàn Institute. Bruxelles, April 18-22,1988

[13] F. FARASSAT and G.P. SUCCI
A review of propeller discrete frequency noise.Prediction technology with emphasis on two current methods for time domain calculations
Journal of Sound and Vibration, 1980, 71, 3, pp.399-419

[14] D. FAVIER,M. NSI MBA,C. BARBI,C. MARESCA
A free wake analysis for hovering rotors and advancing propellers
11th European Rotorcraft Forum, London. Sept.10-13,1985
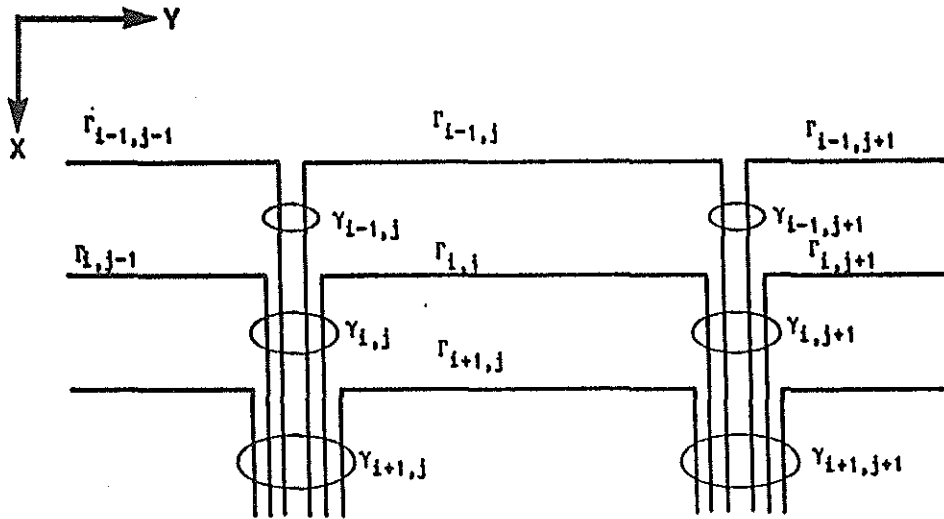
FIG.1 : Sketch for the Vortex Lattice on the blade.
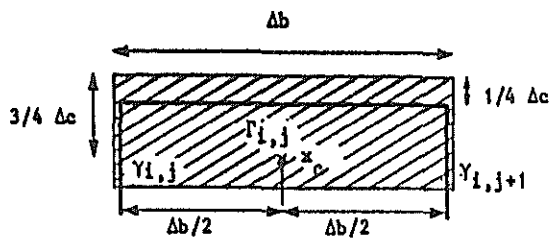
FIG.2 : Position of the vortex line
and the control point.
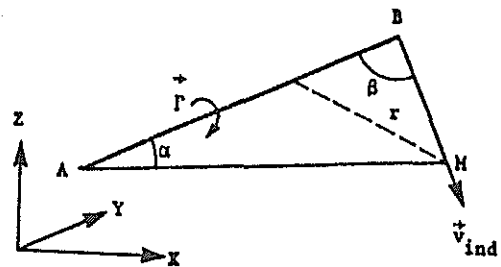
FIG.3 : Induced velocity from a line vortex.

C_T*10000.
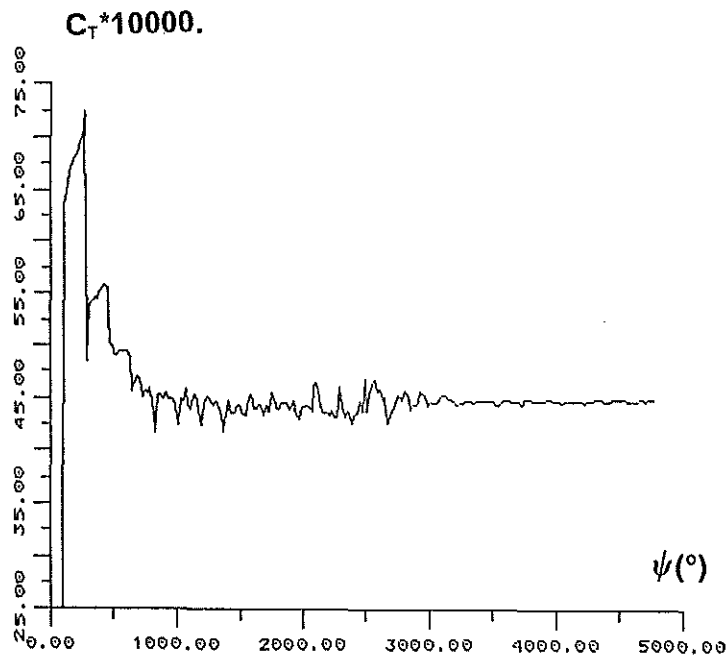
FIG.4 : Evolution of the thrust coefficient for a hovering rotor (collect. pitch
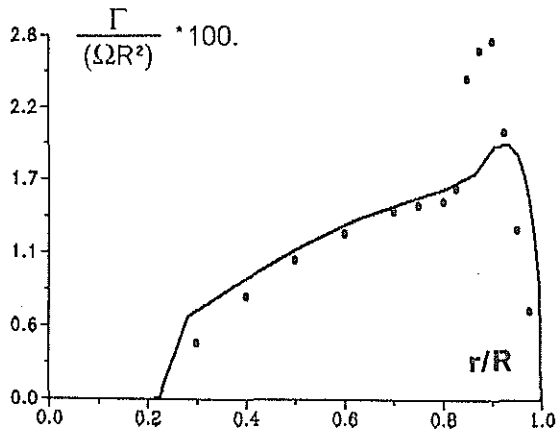10°,coning angle 3°)

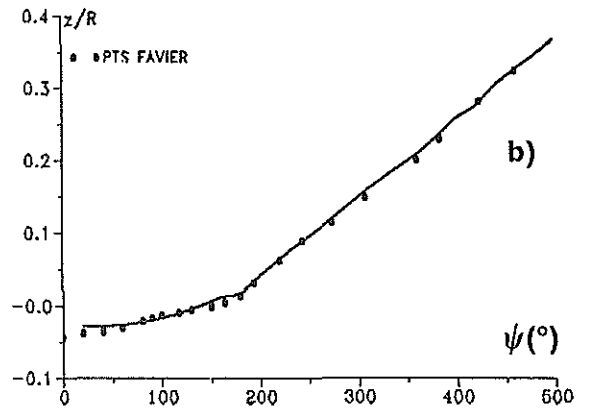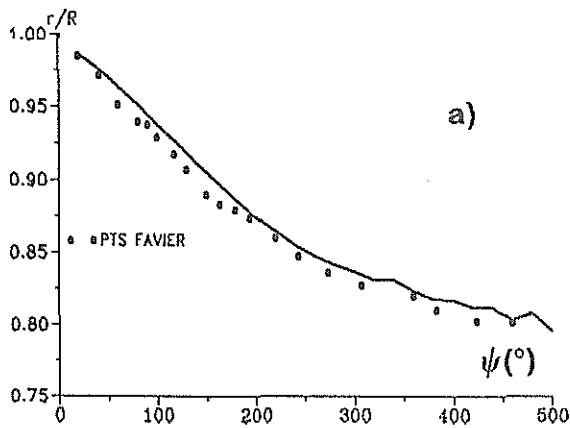FIG.5 : Evolution of the normalized circulation on the blade spar (.experimental points [14])

FIG 6 : Tip vortex Trajectories (solid curve) and experimental points [14]: a) axial coordinates z/R b) contraction of the vortex r/R

C_T*10000.
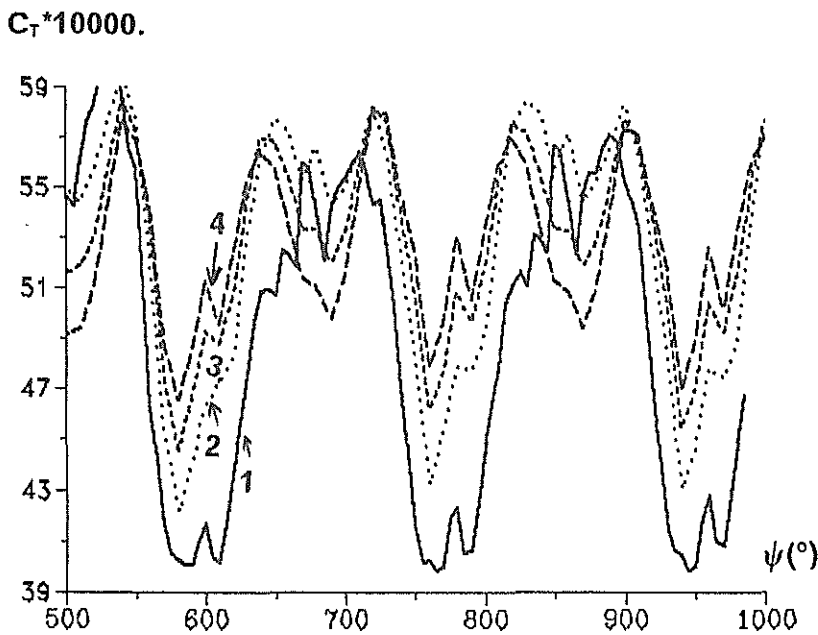
FIG.7 : Influence of the cyclic pitch on the thrust coefficient : 1)No cyclic pitch 2)$\theta_c = 1°97, \theta_s = 1°$ 3)$\theta_c = 2°97, \theta_s = 0.5°$ 4)$\theta_c = 3°5, \theta_s = 0$..
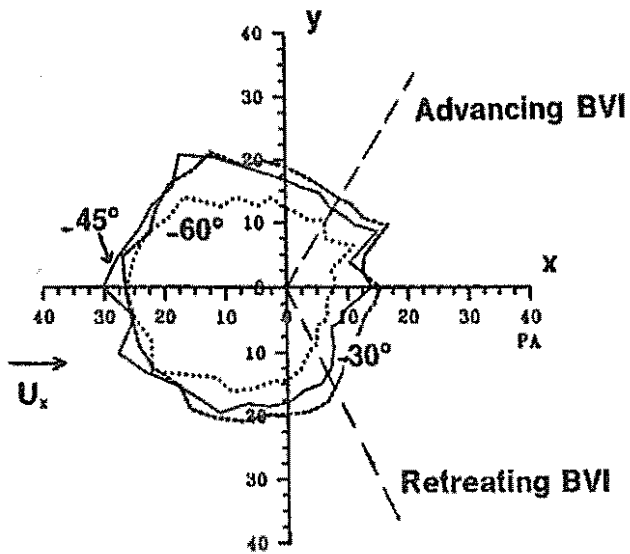
FIG.8 : Horizontal directivities for the BVI noise at 1.72D for 30°,45°,60° below the rotor plane (no cyclic pitch)
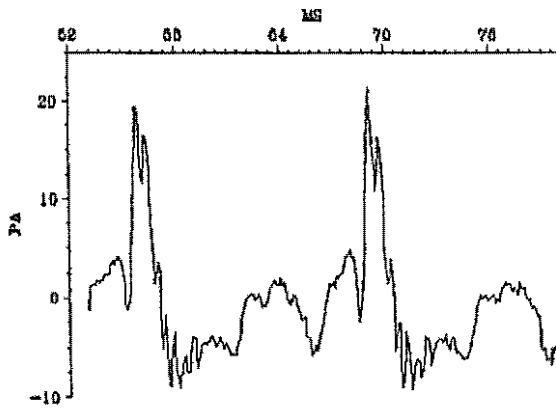
FIG.9 : Pressure signature 30° below the rotor plane for $\theta = 0°$.
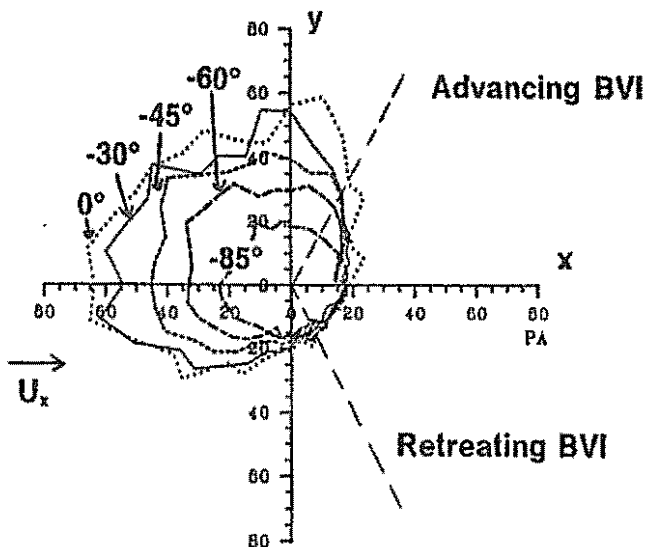
FIG 10 : Horizontal directivities for the loading and thickness noise at 1.72D for $\phi = 0°,-30°,-45°,-60°,-85°$ (with cyclic pitch).
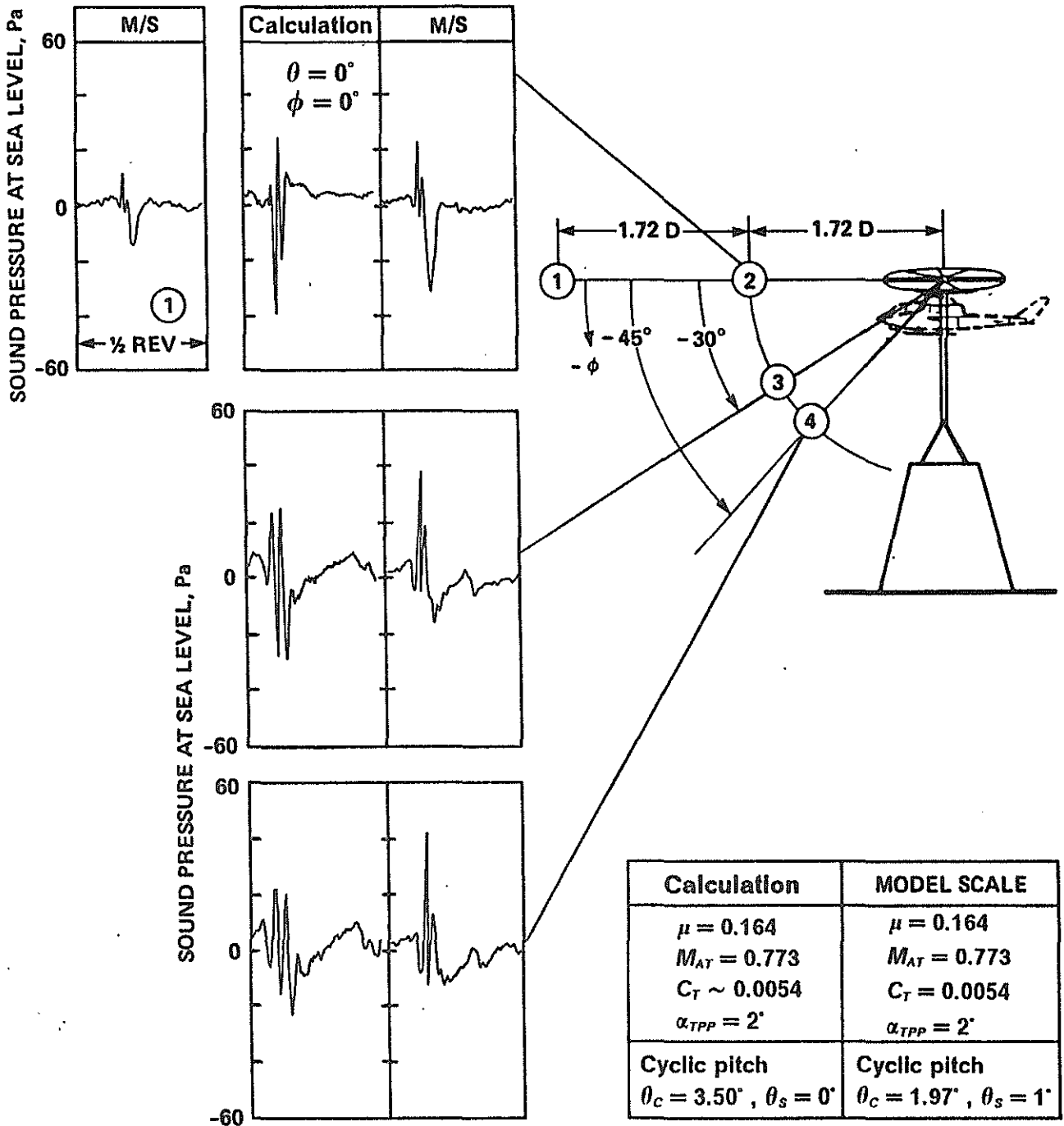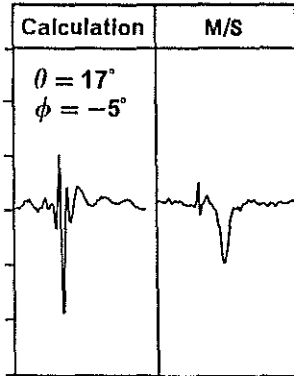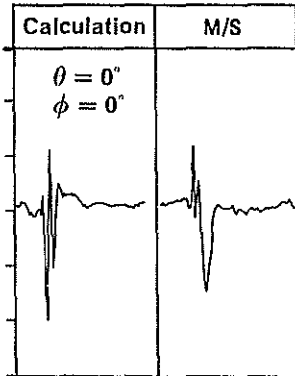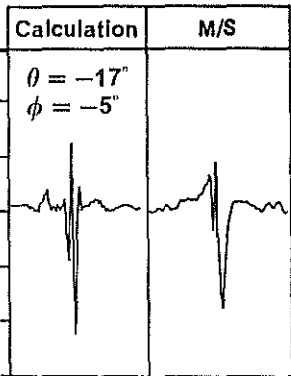
a) Longitudinal directivity

FIG. 11 : Comparison of the present results and model-scale measurements [1] for noise directivity and signatures: a) longitudinal directivity, b) lateral directivity.

IN-PLANE NOISE SIGNATURES

b) Lateral directivity.